Electronic Supplementary Material (ESI) for Soft Matter.

Reconstructing the Mechanical Response of Polybutadiene Rubber Based on Micro-Structural Evolution in Strain-Temperature Space: Entropic Elasticity and Strain-Induced Crystallization as the Bridges

Pinzhang Chen,[a] Yuanfei Lin,[a,b] Jingyun Zhao,[a] Lingpu Meng,[a] Daoliang Wang,[a] Wei Chen*[a] and Liangbin Li[a]

[a.] *National Synchrotron Radiation Laboratory, Anhui Provincial Engineering Laboratory of Advanced Functional Polymer Film, CAS Key Laboratory of Soft Matter Chemistry, University of Science and Technology of China, Hefei, China.*

[b.] *South China Advanced Institute for Soft Matter Science and Technology, South China University of Technology, Guangzhou 510640, China.*

1. Differential Scanning Calorimetry (DSC) Results

The thermal properties of samples were investigated in a nitrogen atmosphere in the temperature range from 25 to -150 °C with the cooling and heating rates of 10 °C / min using a TA Q2000 series DSC instrument. Samples are kept at different temperatures for 10 minutes and then heated up. As shown in Fig. S1(a), clear melting peaks appear below -45 °C. Thus, an uncertain crystallization temperature is defined as T^*. T_g = -110 °C as shown in Fig. S1(b).

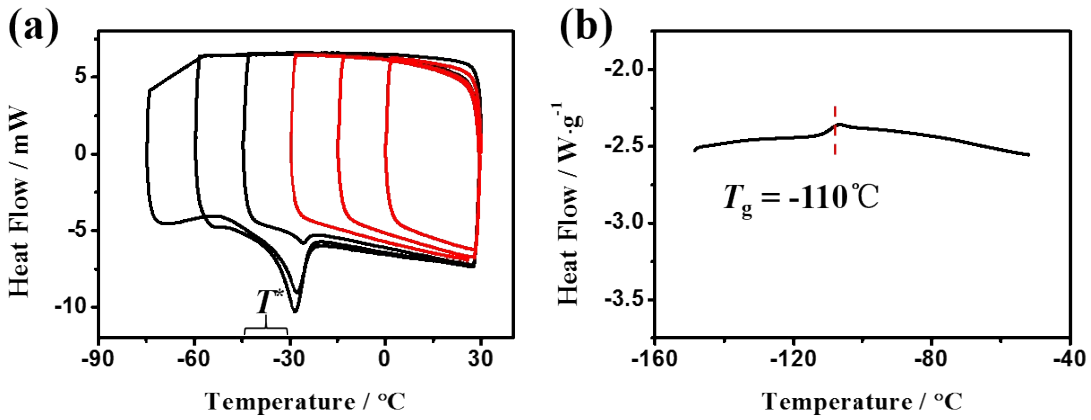

Fig. S1 DSC curves of BR sample acquired at a heating rate of 10 °C/min.

2. Data Analysis

Orientation of the Amorphous Component. Two circles signed in Fig. S2(b) have the same area and intensities of these two circles are defined as I_a(equator) and I_a(meridian), respectively. The orientation ratio of the amorphous part (O_a) is defined through Eq. (1).

$$O_a(\%) = \frac{I_a(equator) - I_a(meridian)}{I_a(equator)} \times 100\% \qquad (1)$$

Crystallinity. It is often difficult to fit one-dimensional integral curve when the crystallinity is small. The crystallinity χ_c is quantitively obtained through the multi-peak deconvolution of the 1D SR-WAXD cures as shown in Fig. S1(c). Areas of three distinct diffraction peaks, assigned to (020), (021) and (110) planes, are defined as A_1, A_2 and A_3, respectively (the second grey shaded area represents the sum of A_2 and A_3). The calculation of χ_c can be described as follows (-30 to 0 °C):

$$\chi_c(\%) = \frac{A_1 + A_2 + A_3}{A_{total}} \times 100\% \qquad (2)$$

where A_{total} is the whole area of the 1D intensity curve in Fig. S2(c).

Onset of SIC. Different from the SR-WAXD patterns at large strain, where clear crystal signal could be distinguished visually, it is hard to find the onset pattern at low strain owing to low crystallinity. The onset of SIC is determined by the azimuthal integration within the range of 180 ° ± 20 ° as shown in Fig. S2(d). And the two-theta range of the azimuthal integration is 14.5 ° to 16.0 °. At 0 °C, for example, a clear azimuthal integration peak appears at $\varepsilon = 2.05$, which is assigned as the onset strain of SIC.

Lateral Crystallite Size. To evaluate the variations of lateral crystallite size, the full widths at half maximum (FWHM, β) of the (020), (021) and (110) planes were estimated. The intensity distribution on the equator was extracted from the original SR-WAXD pattern and each peak was fitted with Gaussian function. After gathering each lattice plane's peak position (2θ) and β, the lateral crystallite size was estimated by using the Scherrer equation as follows:

$$L_{hkl} = \frac{K\lambda}{\sqrt{{\beta_{hkl}}^2 - {\beta_0}^2}cos\theta} \qquad (3)$$

where L_{hkl} is the lateral crystallite size in the direction perpendicular to the (hkl) plane, λ is the wavelength and β_0 is the instrument broadening factor. In this study, the value 0.89 was tentatively used for K and 0.203 ° for β_0.[1, 2]

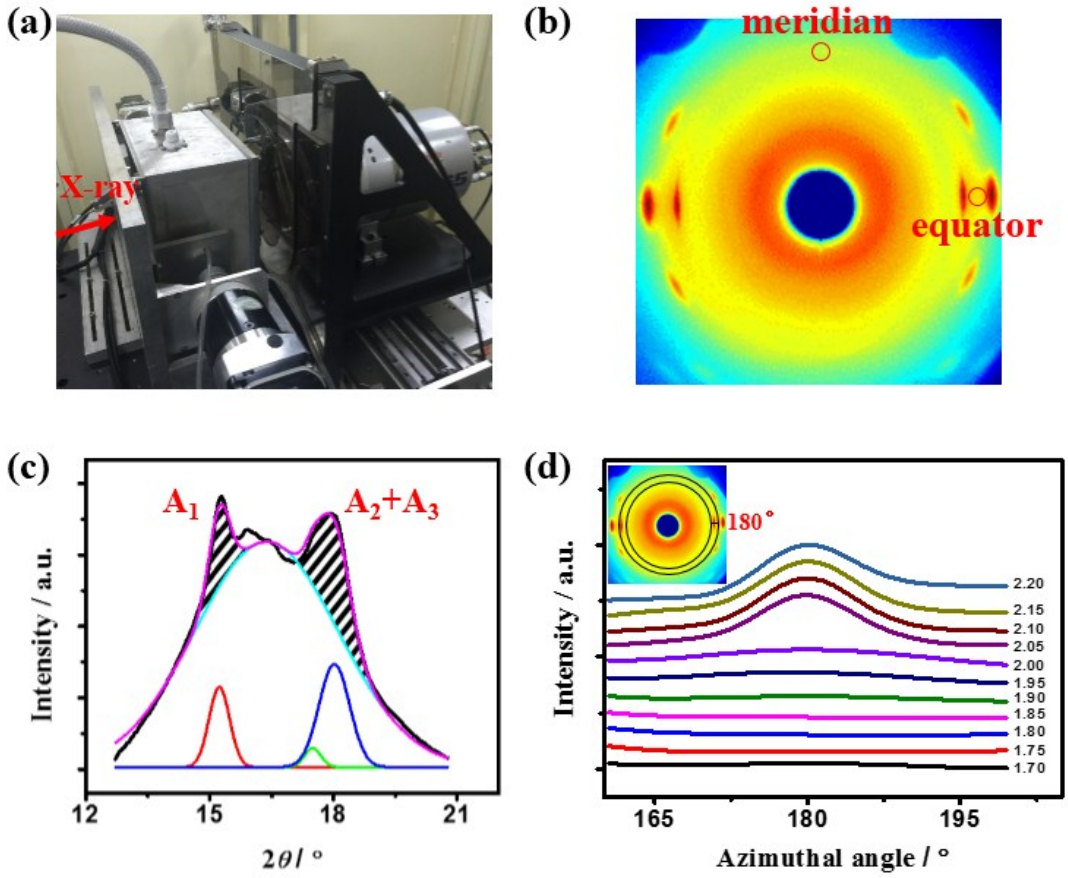

Fig. S2 (a) The low-temperature extensional rheometer mounted at BL16B, SSRF; (b) The SR-WAXD pattern of BR at large strain (ε = 3.0); (c) Peaks fitting of one-dimensional (1D) intensity-2θ curve; (d) Azimuthal integration at equatorial direction stretching at 0 °C.

3. Extension-Retraction Experiment

In order to verify the series-parallel model in BR, an in-situ extension-retraction experiment was also taken. The SR-WAXD measurements were also conducted at beamline BL16B in SSRF and all the experimental parameters were the same with the tensile-fracture experiment except using the Pilatus 2M detector. Considering that the structural evolution regions are different when stretching at different temperatures, the

value of retraction strain ε was set as 2.1 according to Fig. 6.

When retracting at $\varepsilon = 2.1$, the BR crystal disappears at $\varepsilon = 0.45$ at -15 °C but the sample could not shrink at -45 °C after removing the external force. It suggests that the crystal network nearly have no elasticity in that this network is hard to disappear even there exists no external force. And this result is similar to that in NR.

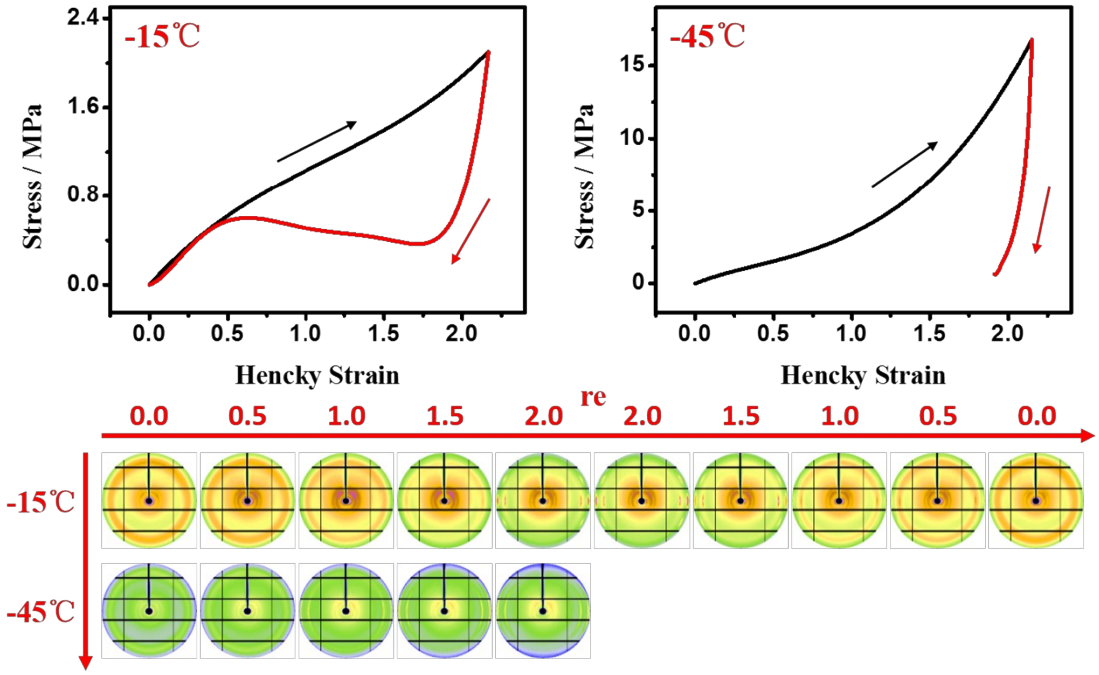

Fig. S3 Sequential evolution of 2D SR-WAXD patterns during extension-retraction at -15 and -45 °C. The tensile direction is vertical

4. Contrast of Different Tensile Methods

The tension device used in most rubber SIC studies is the universal testing machine. Considering that the sample will be restricted by the two clamps in the direction perpendicular to the drawing direction when drawing, all the tensile experiments in the main article are using the low-temperature extensional rheometer.[3] In order to determine which method is more suitable for reconstructing mechanical curves, two

stress-strain curves stretching at room temperature are shown in Fig. S4. Reproducing of the initial stress-elongation ratio curve of BR at room temperature based on Flory's theory is also shown in Fig. S4. The coincidence of the two curves is not as good as that using the extensional rheometer. To ensure the accuracy of the two kinds of strain conversion, *in-situ* CCD experiments were carried out to verify the results (Fig. S5). The results show that there is no sample slippage on the clamps during deformation by using the low-temperature extensional rheometer. (Note: In the case of larger strain, the low-temperature extensional rheometer does have the phenomenon of sample slipping, which results in a greater value of elongation at break.)

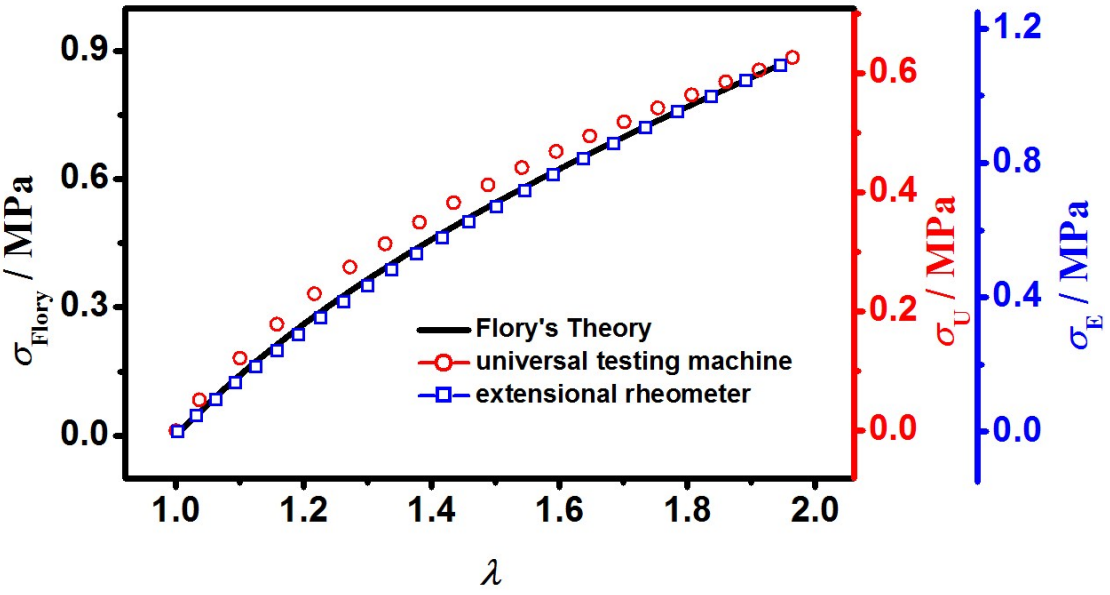

Fig. S4 Stress-strain curves stretching at room temperature using two tensile methods (blue curve represents the stress-strain curve using extensional rheometer while the red one represents that of universal testing machine); The black line means the reproducing of the initial stress-elongation ratio curve of BR at room temperature based on the Flory's theory.

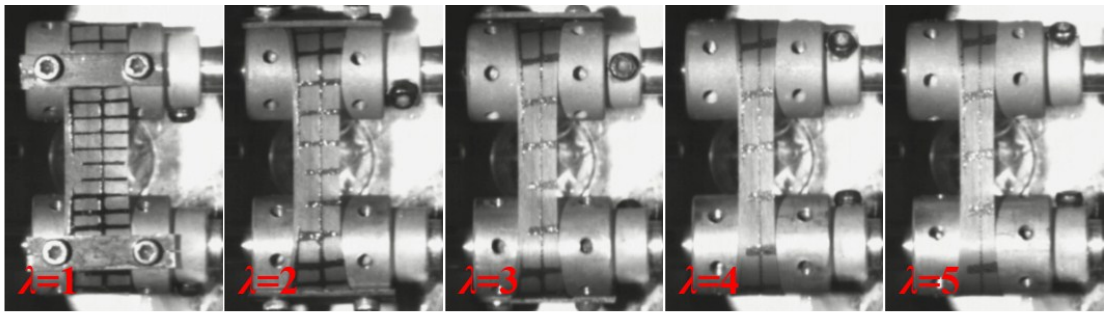

Fig. S5 *In-situ* CCD experiments (The red font in the left lower corner represents the stretch ratio).

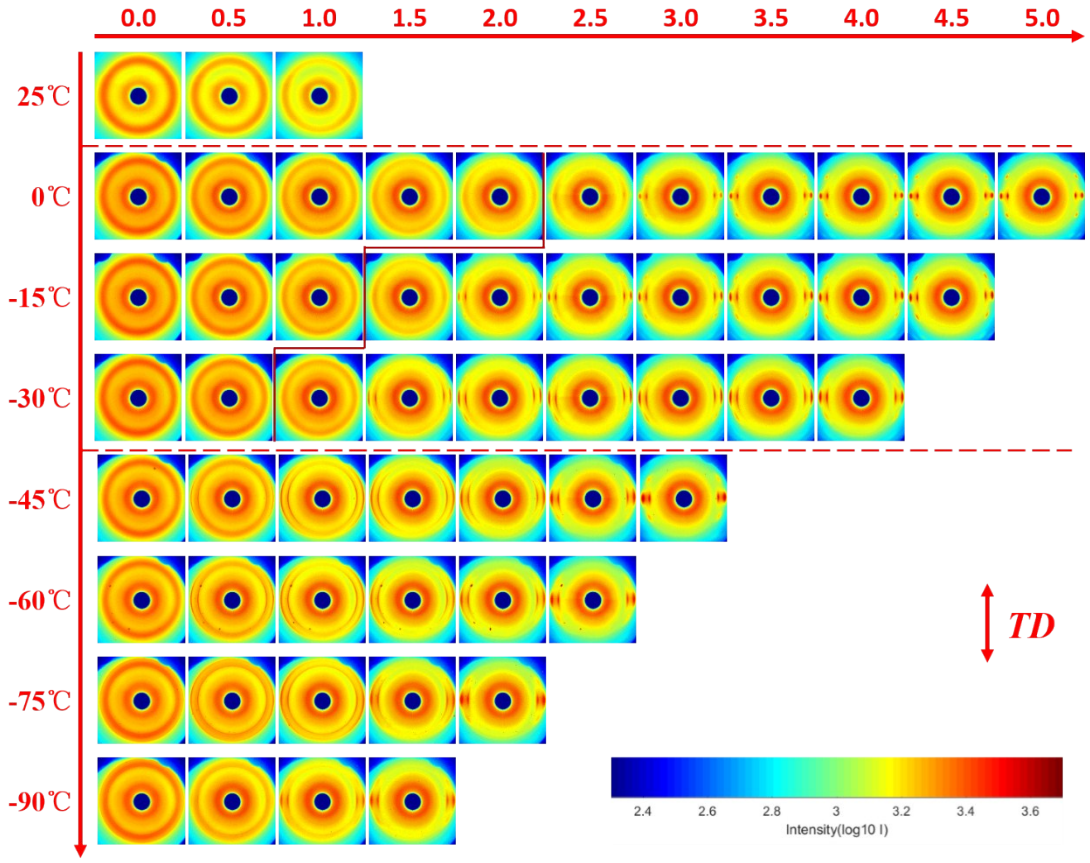

Fig. S6 Sequential evolution of 2D SR-WAXD patterns during uniaxial stretching at different temperatures. Magnified **Fig. 3**.

The data during the stretching process at -45 °C is taken as examples for determining the boundary of the regions in Fig. 4. Both the crossover point of two

tangents and the turning point of the 1st derivative of the crystallinity curve could give the boundary of region II' and III. The starting point of the platform region (region IV) could be defined as the boundary of region III and IV.

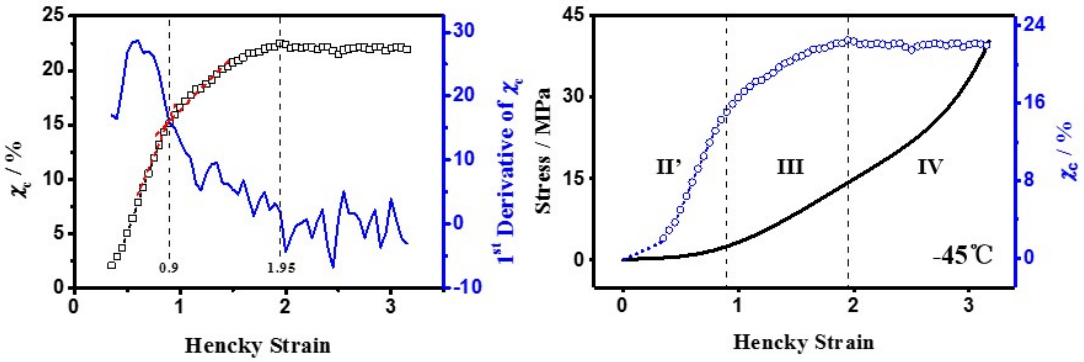

Fig. S7 1st derivative of the crystallinity curve stretching at -45 °C.

5. Notes and references

1 P. Chen, J. Zhao, Y. Lin, J. Chang, L. Meng, D. Wang, W. Chen, L. Chen and L. Li, *Soft Matter*, 2019, **15**, 734-743.

2 P. Chen, Y. Lin, J. Zhao, J. Chang, X. Chen, L. Meng, D. Wang and W. Chen, *Soft Matter*, 2019, **15**, 4363-4370.

3 J. Meissner, *Transactions of the Society of Rheology*, 1972, **16**, 405-420.